PERGAMON

Chemical Engineering Science 58 (2003) 3115–3129

Chemical Engineering Science

www.elsevier.com/locate/ces

Estimation and control of surface roughness in thin film growth using kinetic Monte-Carlo models

Yiming Lou, Panagiotis D. Christofides*

Department of Chemical Engineering, University of California, 405 Hilgard Avenue Box 951592, Los Angeles, CA 90095-1592, USA

Received 16 September 2002; received in revised form 13 December 2002; accepted 26 March 2003

Abstract

In this work, we present an approach to estimation and control of surface roughness in thin film growth using kinetic Monte-Carlo (MC) models. We use the process of thin film growth in a stagnation flow geometry and consider atom adsorption, desorption and surface migration as the three processes that shape film micro-structure. A multiscale model that involves coupled partial differential equations (PDEs) for the modeling of the gas phase and a kinetic MC simulator, based on a high-order lattice, for the modeling of the film micro-structure, is used to simulate the process. A roughness estimator is constructed that allows computing estimates of the surface roughness at a time-scale comparable to the real-time evolution of the process using discrete on-line roughness measurements. The estimator involves a kinetic MC simulator based on a reduced-order lattice, an adaptive filter used to reduce roughness stochastic fluctuations and an error compensator used to reduce the error between the roughness estimates and the discrete roughness measurements. The roughness estimates are fed to a proportional-integral (PI) controller. Application of the proposed estimator/controller structure to the multiscale process model demonstrates successful regulation of the surface roughness at the desired value. The proposed approach is shown to be superior to PI control with direct use of the discrete roughness measurements. The reason is that the available measurement techniques do not provide measurements at a frequency that is comparable to the time-scale of evolution of the dominant film growth dynamics.

Keywords: Thin film growth; Multiscale modeling; Model-based estimation; Feedback control

1. Introduction

Deposition of thin films from gas phase precursors has great industrial importance. The modern integrated circuit technology depends strongly on the uniformity and micro-structure of deposited thin films (Granneman, 1993). Due to the increasingly stringent requirements on the quality of such films including uniformity, composition and micro-structure and the desire to improve productivity by increasing wafer dimensions and reducing product variability, real-time feedback control of thin film deposition becomes important. These trends have motivated significant research efforts on feedback control of film deposition processes with emphasis on control of film spatial uniformity in rapid thermal chemical vapor deposition (e.g., Baker & Christofides, 1999; Theodoropoulou, Adomaitis, & Zafiriou, 1999) and plasma-enhanced chemical vapor deposition (e.g., Armaou & Christofides, 1999). From a control point of view, film spatial uniformity control is a distributed control problem that can be addressed on the basis of continuum-type transport-reaction models by using controller design methods for nonlinear parabolic partial differential equations (PDEs); see the book (Christofides, 2001) for results and references on this problem.

In addition to achieving spatially uniform deposition of thin films, one would like to control film properties such as micro-structure and composition that characterize film quality. This is motivated by the strong dependence of the electrical and mechanical properties of thin films on their micro-structure and composition (see, for example, Lee, Kim, Ju, & Oh, 1999; Chang et al., 2001; Akiyama, Imaishi, Shin, & Jung, 2002). A typical example of thin film growth where feedback control of film surface roughness could be useful is the deposition of thin films of materials with high dielectric constant (such as ZrO_2); such materials are expected to replace SiO_2 thin films to achieve higher

* Corresponding author. Tel.: +1-310-794-1015; fax: +1-310-206-4107.
E-mail address: pdc@seas.ucla.edu (P. D. Christofides).

0009-2509/03/$ - see front matter © 2003 Elsevier Ltd. All rights reserved.
doi:10.1016/S0009-2509(03)00166-0

performance and lower static-power operation in complementary metal oxide semiconductor (CMOS) devices (Chang et al., 2001). In this application, a rough ZrO_2 film surface would lead to silicidation of the interface between the ZrO_2 film and the polysilicon gate during rapid thermal annealing (Chabal et al., 2002), which, in turn, would lead to an interfacial layer with low dielectric constant that would reduce the effective capacity of the gate dielectric (Wallace & Wilk, 2002). Therefore, good control of surface roughness in the deposition of the ZrO_2 thin film is needed to achieve a smoother film surface with fewer reaction sites, which would result in a suppression of the interfacial reactions. The study of feedback control of surface roughness is also motivated by the possibility to obtain roughness measurements in real time using scanning tunneling microscopy (Voigtländer, 2001), spectroscopic ellipsometry (Zapien, Messier, & Collin, 2001) or by combination of on-line measurement techniques for measuring gas phase compositions with off-line measurement techniques for measuring surface roughness. An implementation of the latter approach was recently carried out by Ni, Lou, Christofides, Lao, and Chang (2003), where it was used to measure carbon composition of thin films in plasma-enhanced chemical vapor deposition using combination of optical emission spectroscopy (OES) and X-ray photoelectron spectroscopy (XPS).

While deposition uniformity control can be accomplished on the basis of continuum-type distributed models, precise control of film properties requires models that predict how the film state (microscopic scale) is affected by changes in controllable process parameters (macroscopic scale). The desire to understand and control the micro-structure of thin films has motivated extensive research on fundamental mathematical models describing thin film growth and its interactions with the surrounding gas. Thin film deposition is a typical process including multiple time and length scales and this has motivated the use of multiscale models to obtain manageable modeling descriptions. Specifically, one approach to model thin film growth is to model the chamber-scale phenomena using a set of PDEs derived from mass, momentum and energy balances, and to model the micro-configuration of the surface using the kinetic Monte Carlo (MC) method (Vlachos, 1997; Lam & Vlachos, 2001). The two models are coupled through the surface boundary conditions. Other approaches have been also developed to study the growth of thin films using the level set method (Chen et al., 2001). While multiscale modeling provides a computationally attractive alternative with respect to direct modeling of the entire reactor using a molecular model, it still leads to dynamic models that cannot be solved fast enough for real-time estimation and control purposes.

Mathematically, kinetic MC methods provide a numerical solution to the master equation (Kang & Weinberg, 1992), which is a stochastic differential equation describing the evolution of probabilities that the thin film is at a certain micro-configuration. As the lattice size in the MC simulation increases, thin film properties computed from the kinetic MC simulation converge to the expected properties obtained from the master equation, which are quantities to be controlled. As an alternative with respect to closed-form process models (e.g., linear or nonlinear systems of differential equations), which are not available for describing the micro-structure of thin films, the kinetic MC method can predict expected properties of thin film micro-structure by explicitly accounting for the micro-processes that directly shape thin film growth. The accuracy of solutions from kinetic MC simulations depends on the size of the lattice used in the simulation which, in turn, determines the computational requirements of the simulation. The computational requirements for a solution with reasonable accuracy make the direct use of kinetic MC algorithms in an on-line feedback control scheme impossible. Motivated by this, recent research efforts have focused on the development of order reduction techniques for the master equation (Raimondeau & Vlachos, 2000; Gallivan, Goodwin, & Murray, 2001; Gallivan & Murray, 2003). Other approaches have also been developed to identify linear models from outputs of kinetic Monte Carlo simulators and perform controller design by using linear optimal control theory (Armaou, Siettos, & Kevrekidis, 2002).

In this work, we present an approach to estimation and control of surface roughness in thin film growth using kinetic MC models. We use the process of thin film growth in a stagnation flow geometry and consider atom adsorption, desorption and surface migration as the three processes that shape film micro-structure. A multiscale model that involves coupled PDEs for the modeling of the gas phase and a kinetic MC simulator, based on a high-order lattice, for the modeling of the film micro-structure, is used to simulate the process. A roughness estimator is constructed that allows computing estimates of the surface roughness at a time-scale comparable to the real-time evolution of the process using discrete on-line roughness measurements. The estimator involves a kinetic MC simulator based on a reduced-order lattice, an adaptive filter used to reduce roughness stochastic fluctuations and an error compensator used to reduce the error between the roughness estimates and the discrete roughness measurements. The roughness estimates are fed to a PI controller. Application of the proposed estimator/controller structure to the multiscale process model demonstrates successful regulation of the surface roughness at the desired value. The proposed approach is shown to be superior to PI control with direct use of the discrete roughness measurements. The reason is that the available measurement techniques do not provide measurements at a frequency that is comparable to the time-scale of evolution of the dominant film growth dynamics.

2. Process description

We consider the growth of a thin film from a fluid in a vertical, stagnation flow geometry. The process is shown in

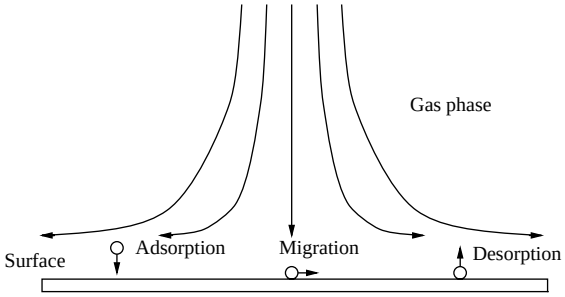

Fig. 1. Illustration of the thin film growth process.

Fig. 1. In this geometry, inlet fluid flow forms a uniform boundary layer adjacent to the surface of the substrate and precursor atoms diffuse through the boundary layer and deposit a uniform thin film on the substrate (Gadgil, 1993). Upon arrival on the surface, the precursor atoms are adsorbed onto the surface. Subsequently, adsorbed atoms may desorb to the gas phase or migrate on the surface.

From a modeling point of view, the major challenge is the integration of the wide range of length and time-scales that the process encompasses (Vlachos, 1997). Specifically, in the gas phase, the processes of heat/mass transport can be adequately modeled under the hypothesis of continuum, thereby leading to PDE models for chamber temperature and species concentration. However, when the micro-structure of the surface is studied, microscopic events such as atom adsorption, desorption and migration have to be considered, and the length-scale of interest reduces dramatically to the order of that of several atoms. Under such a small length scale, the continuum hypothesis is no longer valid and deterministic PDEs cannot be used to describe the microscopic phenomena. Different approaches, such as MC simulation or molecular dynamics, should be employed to model the evolution of surface micro-structure.

Although different modeling approaches are used to model the macroscopic and microscopic phenomena of the process, there are strong interactions between the macro- and micro-scale phenomena. For example, the concentration of the precursor in the inlet gas governs the rate of adsorption of atoms on the surface, which, in turn, influences the surface roughness. On the other hand, the density of the adatoms on the surface affects the rate of desorption of atoms from surface to the gas phase, which, in turn, influences the gas phase concentration of the precursor. A multiscale model (Vlachos, 1997) is employed in this work to capture the evolution of both macroscopic and microscopic phenomena of the thin film growth process as well as their interactions. A set of PDEs derived from the mass, momentum and energy balances are used to describe the gas phase dynamics. Kinetic MC simulation (Fichthorn & Weinberg, 1991) is employed to capture the evolution of surface micro-structure. Furthermore, the parameters of MC simulation such as the temperature and precursor concentration are provided by the solution of PDEs, and the results from the kinetic MC simulation are used to determine the boundary conditions of the PDEs of the macroscopic model.

3. Gas phase model

Under the assumption of axisymmetric flow, the gas phase can be modeled through continuum-type momentum, energy and mass balances as follows (Lam & Vlachos, 2001):

$$\frac{\partial}{\partial\tau}\left(\frac{\partial f}{\partial\eta}\right)=\frac{\partial^3 f}{\partial\eta^3}+f\frac{\partial^2 f}{\partial\eta^2}+\frac{1}{2}\left[\frac{\rho_b}{\rho}-\left(\frac{\partial f}{\partial\eta}\right)^2\right], \tag{1}$$

$$\frac{\partial T}{\partial\tau}=\frac{1}{P_r}\frac{\partial^2 T}{\partial\eta^2}+f\frac{\partial T}{\partial\eta}, \tag{2}$$

$$\frac{\partial y_i}{\partial\tau}=\frac{1}{Sc_j}\frac{\partial^2 y_i}{\partial\eta^2}+f\frac{\partial y_i}{\partial\eta}. \tag{3}$$

The following boundary conditions are used for $\eta\to\infty$:

$$T=T_{\text{bulk}},$$

$$\frac{\partial f}{\partial\eta}=1,$$

$$y_j=y_{jb},\quad j=1,\ldots,N_g \tag{4}$$

and for $\eta\to 0$ (surface):

$$T=T_{\text{surface}},$$

$$f=0,$$

$$\frac{\partial f}{\partial\eta}=0,$$

$$\frac{\partial y_j}{\partial\eta}=0\quad \text{for } j\neq \text{growing},$$

$$\frac{\partial y_{\text{growing}}}{\partial\eta}=\frac{Sc_{\text{growing}}(R_a-R_d)}{\sqrt{2a\mu_b\rho_b}}, \tag{5}$$

where f is the dimensionless stream function, R_a and R_d are the rates of adsorption and desorption, respectively, η is the dimensionless distance from the surface, ρ is the density of the mixture, P_r is the Prandtl number, y_j and Sc_j are the mole fraction and Schmidt number of the species j, respectively, T_{bulk} is the temperature of the bulk gas, N_g is the number of total species in the gas phase, μ_b and ρ_b are the viscosity and the density of the bulk, respectively, a is the hydrodynamic strain rate and $\tau=2at$ is the dimensionless time.

Although the macroscopic model describes the spatio-temporal evolution of the precursor concentration and temperature (which influence the configuration of the growing surface), no direct information of the surface micro-structure is available from the macroscopic model. Furthermore, the boundary conditions for the mass transfer equation of the growing species depend on the rates of adsorption and desorption. Therefore, a microscopic model is necessary to model the micro-structure of the surface and

to determine the boundary conditions of the mass transfer equation.

4. Surface micro-structure model

The thin film growth considered in this work encompasses three kinds of processes, the adsorption of atoms from the gas phase to the surface; the desorption of atoms from the surface to the gas phase and the migration of atoms on the surface. The statistical properties of these processes can be studied by sampling a duration t into n identical time intervals δ. When $n \to \infty$, δ will be small enough so that each interval will contain one event at the most. The average of the rate can be defined as (Fichthorn & Weinberg, 1991)

$$r = \lim_{\delta \to 0} \frac{n_\delta}{t}, \tag{6}$$

where n_δ is the number of time intervals containing events. Therefore, the probability that n_e events will occur in time t is

$$P_{n_e} = \binom{n}{n_e} (r\delta)^{n_e}(1 - r\delta)^{n-n_e}, \tag{7}$$

where n is the number of intervals in time duration t and

$$\binom{n}{n_e} = \frac{n!}{n_e!(n - n_e)!}.$$

When $n \to \infty$,

$$P_{n_e} = \frac{rt^{n_e}}{n_e!} \mathrm{e}^{-rt}, \tag{8}$$

which is a Poisson distribution (Van Kampen, 1992). Eq. (8) can be readily applied to the adsorption, desorption and migration processes involved in the thin film growth process. Due to the fact that the ensemble of independent Poisson processes is also a Poisson process (Fichthorn & Weinberg, 1991), the thin film growth process is a Poisson process.

Due to that stochastic nature of the process, the probability that the surface is in the possible configuration α is described by the so-called master equation (Van Kampen, 1992):

$$\frac{\mathrm{d}P_\alpha}{\mathrm{d}t} = \sum_\beta (W_{\alpha\beta}P_\beta - W_{\beta\alpha}P_\alpha), \tag{9}$$

where P_α is the probability of the surface being in configuration α and $W_{\alpha\beta}$ is the transition probability rate of the surface going from configuration β to configuration α, which can be computed from the probability distribution of adsorption, desorption and migration. It is hard to write down the explicit form of Eq. (9) because the number of the possible states is extremely large for most systems of realistic size (Gallivan & Murray, 2003). For example, consider a system of 10×10 sites with a maximum height of 1, the number of configurations is $2^{100} \approx 10^{30}$. This makes the direct solution of Eq. (9), using numerical methods for integration of ODEs (e.g., Runge–Kutta), impossible.

MC methods provide an approach to solve the master equation numerically. To capture the dynamic properties of the system, the MC algorithms must be able to satisfy the detailed balance criterion, appropriately calculate the life time of each MC event and guarantee the independence of events by using an appropriate random number generator (Fichthorn & Weinberg, 1991). The way to satisfy detailed balance criterion differs when different algorithms are used. In general, there are two groups of MC algorithms which have been developed to simulate processes governed by the master equation: (a) the null-event algorithm (Ziff, Gulari, & Barshad, 1986), and (b) the kinetic MC method (Jansen, 1995). When null-event algorithm is used, which tries to execute MC events on randomly selected sites with certain probabilities of success, the probabilities of successful trials should be appropriately constructed to satisfy the detailed balance criterion. On the other hand, if kinetic MC method is used, which selects the MC event before the selection of the site on which the MC event is going to be executed, the detailed balance criterion is satisfied by appropriately constructing the probabilities of the different kinds of MC events to be selected. Upon a successful MC event, the time passed during the event is computed based on the total rates of all the micro-processes (Vlachos, 1997). In this way, the dynamic properties of the system can be captured. Since the kinetic MC method is computationally more efficient than the null-event algorithm, it is used to simulate the surface processes in the thin film growth process in this study (see Reese, Raimondeau, and Vlachos (2001) for a detailed discussion on comparison of computational efficiency of the kinetic MC method to the null-event algorithm).

To run the MC simulation for the evolution of the surface micro-structure, an $N \times N$ lattice is initially constructed. The size of the lattice (or the value of N) is determined based on the desired accuracy and the need to obtain a numerically stable solution. Generally, a larger lattice can achieve higher accuracy (in terms of average properties and size of stochastic fluctuations), but requires larger solution time. When the lattice is ready, microscopic events are executed on the lattice based on the probabilities of the individual processes. To simplify the development, only first nearest-neighbor interactions are considered, the solid-on-solid approximation of a simple cubic lattice is made and periodic boundary conditions are used.

In this study, we consider the multilayer growth and all the sites are available for adsorption at all the time, therefore, the adsorption rate is treated as site independent. For an ideal gas, the adsorption rate is given by the kinetic theory (Lam & Vlachos, 2001):

$$r_a = \frac{s_0 P}{\sqrt{2\pi mkT}C_{\mathrm{tot}}}, \tag{10}$$

where s_0 is the sticking coefficient, k is the Boltzmann constant, P is the partial pressure of the precursor, C_{tot} is the

concentration of sites on the surface, m is the molecular weight of the precursor and T is the gas phase temperature above the surface.

The rate of desorption depends on the local activation energy. Under the consideration of only first nearest-neighbor interactions, the desorption rate of an atom from a surface site with n first nearest neighbors is

$$r_d(n) = v_0 \exp\left(-\frac{nE}{kT}\right), \tag{11}$$

where E is the energy associated with a single bond on the surface and v_0 is the frequency of events, which is determined by the following expression:

$$v_0 = k_{d0} \exp\left(-\frac{E_d}{kT}\right), \tag{12}$$

where k_{d0} is the event frequency constant and E_d is the energy associated with desorption.

Surface migration is modeled as desorption followed by re-adsorption (Gilmer & Bennema, 1972), and the migration rate is given by

$$r_m(n) = v_0 A \exp\left(-\frac{nE}{kT}\right), \tag{13}$$

where A is associated with the energy difference that an atom on a flat surface has to overcome in jumping from one lattice site to an adjacent one and A is given as

$$A = \exp\left(\frac{E_d - E_m}{kT}\right), \tag{14}$$

where E_m is the energy associated with migration.

When the lattice is set and the rates of the three events are determined based on the corresponding rate expressions, a kinetic MC simulation is executed following the algorithm reported by Vlachos (1997). First, a random number is generated to select an event to be run based on the above rates, then, a second random number is generated to select the site where the event will be executed from the list of the sites that the event is possible to happen. Upon an executed event, a time increment dt is computed by Lam and Vlachos (2001)

$$\mathrm{d}t = \frac{-\ln \xi}{r_a \times N_T + v_0(1+A)\sum_{m=1}^{5} N_m \exp(\frac{-mE}{kT})}, \tag{15}$$

where ξ is a random number in the $(0,1)$ interval, N_T is the total number of sites on the lattice and N_m is the number of atoms that have m neighbors on the surface.

5. A roughness estimator

The objective of this section is to present a systematic method for the design of a dynamic estimator to estimate surface roughness in real time using on-line roughness measurements obtained at discrete time instants. Surface roughness is a property of interest from a control point of view since it directly influences device properties. The roughness, r, is represented by the number of broken bonds on the surface (Raimondeau & Vlachos, 2000):

$$r = 1 + \frac{\sum_{i,j}(|h_{i+1,j} - h_{i,j}| + |h_{i-1,j} - h_{i,j}| + |h_{i,j+1} - h_{i,j}| + |h_{i,j-1} - h_{i,j}|)}{2 \times N \times N}, \tag{16}$$

where N is the size of the lattice and $h_{i,j}$ is the number of atoms at site (i,j).

In the kinetic MC simulation, the size of the lattice influences the accuracy of the result and the computational demand. Roughly speaking, the computational complexity of the algorithm we adopt in this work is $O(N^4)$, and the magnitude of the fluctuation in the solution is $O(1/N^2)$, where N is the size of the lattice. The 4th order dependence on computational complexity and the 2nd order dependence of fluctuations on the size of the lattice leave room for reducing the solution time with relatively small loss of accuracy.

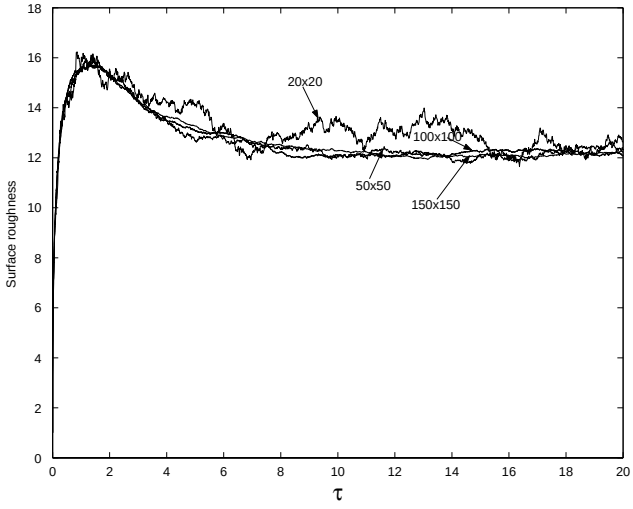

Fig. 2. Comparison of roughness profiles obtained from kinetic MC simulators which use 20×20, 50×50, 100×100, and 150×150 lattices.

Fig. 2 shows the evolution of the surface roughness at $T = 600$ from kinetic MC simulators using different lattice sizes: 20×20, 50×50, 100×100 and 150×150. All the simulation results in this paper are plotted with respect to the dimensionless time τ ($\tau = 2at$, where t is the real time and a is the hydrodynamic strain rate; the value of a used in this work is shown in Table 1.). The result from a kinetic MC simulator which uses a 20×20 lattice contains significant fluctuations compared to the roughness profiles obtained from a kinetic MC simulator which uses a higher-order lattice. However, it gives the same trend of the evolution of surface roughness. Furthermore, the results from kinetic MC simulators which use 50×50, 100×100 and 150×150 lattices are very close, thereby implying that

Table 1
Process and controller parameters

P	10^{-4} atm	a	5 s^{-1}
s_0	0.1	m	0.028 kg/mol
C_{tot}	10^{19} sites/m^2	k_{d0}	10^{13} s^{-1}
E_d	7.14×10^4 J/mol	E_m	4.28×10^4 J/mol
E	7.14×10^4 J/mol	K_0	0.5
K_s	1.0	K_e	0.08
K_c	30	τ_c	0.4
y_{set}	1.5		

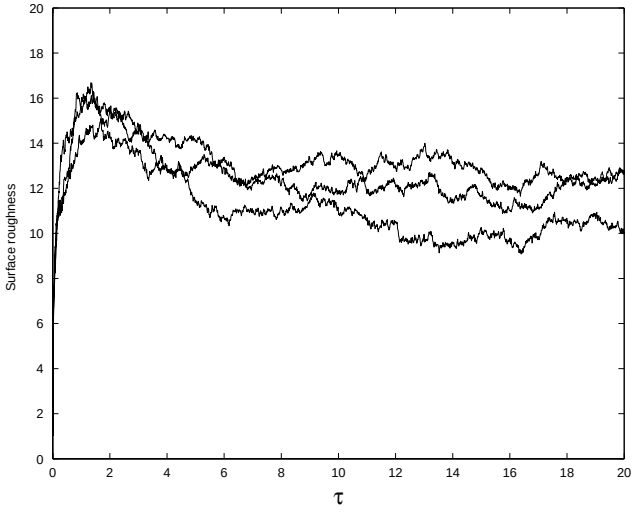

Fig. 3. Comparison of roughness profiles from three independent kinetic MC simulations which utilize a 20×20 lattice.

further increase of the lattice size does not improve the accuracy of the results. Due to the stochastic nature of the algorithm, it is not possible to obtain the same results from repeated runs starting from the same initial conditions (see remark 5 for how to handle this problem). However, for sufficiently large lattice size, the results from different runs are consistent in the sense that they provide surface roughness profiles that are very close. Figs. 3 and 4 show the results from three independent kinetic MC simulations which utilize a 20×20 lattice and a 50×50 lattice. Clearly, as the lattice size increases, the error among different runs decreases.

To implement on-line control of surface roughness, the size of the lattice has to be selected to make the model computations be at a time-scale comparable to the process real-time evolution (see also remark 1 for a discussion on the issue of selecting the size of the reduced-order lattice). In our simulations, when the size of the lattice is reduced to 20×20, the time of simulation is comparable to the real-time process evolution. To overcome the fluctuations introduced by the smaller lattice size, a second-order linear filter is used to reject the noise in the roughness values obtained from the kinetic MC simulator, which uses a reduced-order lattice

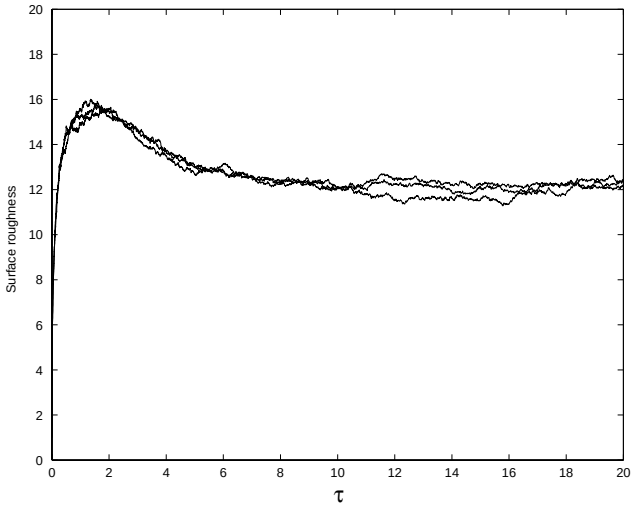

Fig. 4. Comparison of roughness profiles from three independent kinetic MC simulations which utilize a 50×50 lattice.

model here with the following state space representation:

$$\frac{d\hat{y}_r}{d\tau} = y_1,$$

$$\frac{dy_1}{d\tau} = \frac{K}{\tau_I}(y_r - \hat{y}_r) - \frac{1}{\tau_I} y_1, \tag{17}$$

where y_r is the output of the kinetic MC simulator which uses a reduced-order lattice and $\hat{y}_r$ is the filter output, K is the filter gain and τ_I is the time constant. To accelerate the response of the filter and avoid overshoot, $\tau_I = 0.5/K$.

Due to the Arrhenius-like dependence of the rate of desorption and surface migration on temperature, the dynamics of the roughness with respect to temperature variations is very fast. To this end, we need a filter that can both track the fast dynamics and reject the noise so that the noise will not deteriorate the controller performance. However, fast tracking and efficient noise rejection are two conflicting objectives that are very hard to be achieved simultaneously. Fortunately, during the fast dynamic stage, the roughness is very large compared to the fluctuations and the effect of the fluctuations on the controller performance is insignificant. The fluctuations begin to deteriorate the controller performance significantly only when the controlled roughness is close to the set-point value. Motivated by this, an adaptive scheme is used to determine the gain of the filter on-line such that the filter focuses on tracking the growth dynamics ie. $\hat{y}_r$ is close to y_r at the fast dynamic stage and on noise rejection when the surface dynamics slow down. To achieve this, the gain of the filter is adjusted according to the following law:

$$K(\tau) = K_0 \frac{\left| \int_{\tau-\Delta\tau}^{\tau} y_r(t)\,dt - \int_{\tau-2\Delta\tau}^{\tau-\Delta\tau} y_r(t)\,dt \right|}{\Delta\tau^2} + K_s, \tag{18}$$

where K_0 is a constant, K_s is the steady-state gain for the adaptive filter and $\Delta\tau$ is the dimensionless time interval

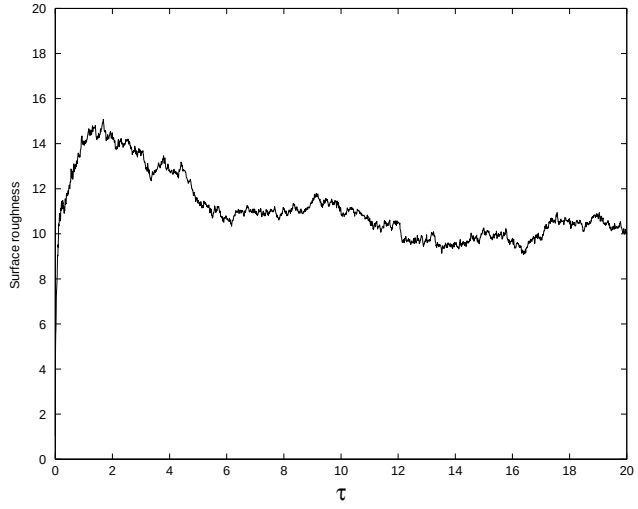

Fig. 5. Evolution of the roughness obtained directly from a kinetic MC simulator which uses a 20×20 lattice.

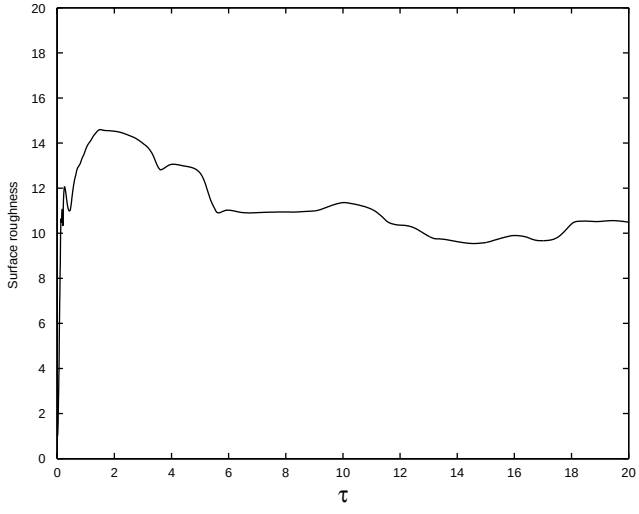

Fig. 6. Filtered roughness from a kinetic MC simulator which uses a 20×20 lattice.

between two updates of K. To make the filter focus on tracking the growth dynamics at the fast dynamic stage and on noise rejection when the surface dynamics slow down, the K_0 and K_s in Eq. (18) are tuned such that the first term in the right-hand side of Eq. (18) is dominant during the fast dynamics stage and the second term in the right-hand side of Eq. (18) is dominant when the dynamics slow down. The filter parameters (K_0 and K_s) are determined from process step tests and are shown in Table 1. Regarding the choice of $\Delta\tau$, although a better tracking performance is expected when a smaller $\Delta\tau$ is used, a very small $\Delta\tau$ will introduce the effect of fluctuations on the filter gain and should be avoided. Fig. 5 shows the roughness obtained directly from a kinetic MC simulator using a 20×20 lattice and Fig. 6 shows the roughness from the same kinetic MC simulator and the adaptive filter. The results clearly show that the adaptive filter can

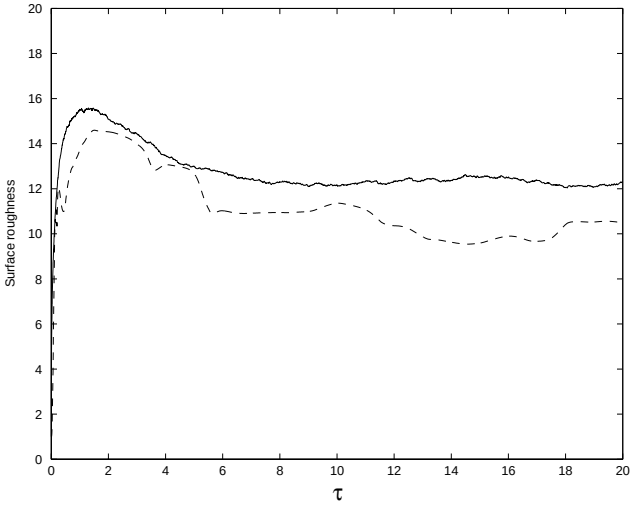

Fig. 7. Filtered roughness from a kinetic MC simulator which uses a 20×20 lattice (dashed line) and roughness from a kinetic MC simulator which uses a 100×100 lattice (solid line).

reject most of the fluctuation in the roughness values while capturing the characteristics of the output of the kinetic MC simulator which uses the reduced-order lattice.

The significant fluctuation is not the only problem need to be fixed when a reduced-order lattice is used in the kinetic MC simulator. There is also model inaccuracy when the outputs of kinetic MC simulators, which use a reduced-order lattice and a high-order lattice, are compared. Fig. 7 shows the output from a kinetic MC simulator which uses a 20×20 lattice after passing the filter and that from a kinetic MC simulator which uses a 100×100 lattice. Although the filtered roughness from the kinetic MC simulator which uses a reduced-order lattice contains little fluctuation, the overall profile does not match that of the kinetic MC simulator which uses a high-order lattice. This can be corrected by using a measurement error compensator that uses the available roughness measurements obtained from a kinetic MC simulator which uses the high-order lattice model to produce an improved roughness estimate. The state-space representation of the measurement error compensator is of the following form

$$\frac{\mathrm{d}e}{\mathrm{d}\tau} = K_e(y_h(\tau_{m_i}) - \hat{y}(\tau_{m_i})); \quad \tau_{m_i} < \tau \leqslant \tau_{m_{i+1}}; \;\; i = 1, 2, \ldots \tag{19}$$

and the final roughness estimates are computed by

$$\hat{y} = \hat{y}_r + e. \tag{20}$$

In the above equations, K_e is the compensator gain, e is the estimated model error, which is used to compensate the model output, $\hat{y}$ is the roughness estimate, $\hat{y}_r$ is the filtered output from a kinetic MC simulator which uses a reduced-order lattice and y_h is the output of a kinetic MC

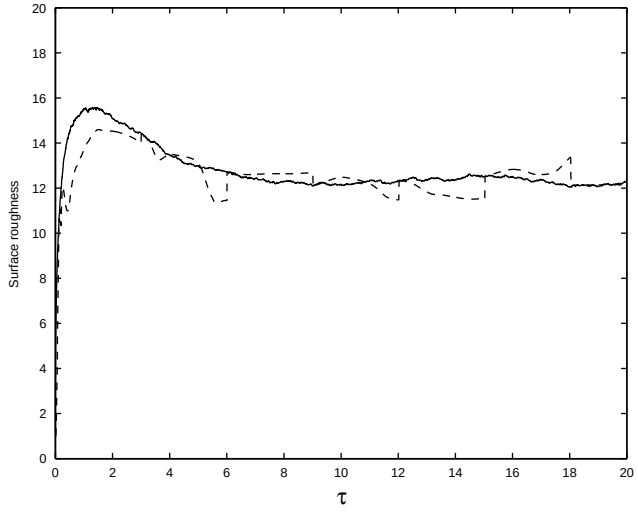

Fig. 8. Roughness profiles from the roughness estimator based on a 20×20 lattice (dashed line) and from a kinetic MC simulator which uses a 100×100 lattice (solid line).

simulator which uses the high-order lattice (in an experimental set-up y_h could be obtained from the measurement sensor). Since the roughness measurements are only available at discrete points in time $\tau_m = [\tau_{m_1}, \tau_{m_2}, \dots]$, the right-hand side of Eq. (19) is computed at the time in which a roughness measurement is available and is kept in this value in the time interval between two available roughness measurements.

The combination of the adaptive filter and the measurement error compensator functions as a roughness estimator, which is capable to accurately predict the evolution of roughness during the thin film growth by using measurements of the precursor concentration above the substrate and surface roughness. In this work, we assume that the estimate of precursor concentration above the substrate is available; the estimation of surface precursor concentration can be done by using estimation methods for continuum-type PDE models (Christofides, 2001). Fig. 8 illustrates the prediction of surface roughness by the roughness estimator based on a 20×20 lattice and its comparison to the output from the kinetic MC model which uses a high-order lattice. The results clearly show that when measurements are used, the estimator based on a kinetic MC simulator which uses a reduced-order lattice can predict the evolution of surface roughness, while the computational requirements are kept within the limit that makes on-line control possible.

Remark 1. It is important to point out that while a 20×20 reduced-order lattice captures adequately the evolution of the surface roughness in this specific thin film growth process, the dimension of the reduced-order lattice in general should be chosen so that the interactions between the surface atoms are adequately captured, and also that it is large enough to describe the spatio-temporal phenomena occurring (e.g., island formation) on the surface. The choice of the dimension of the reduced-order lattice can be guided by the study of the surface behavior obtained by simulating a very high order lattice; in this way, the proposed approach, based on reduction of lattice size, appears to be quite intuitive (see Gallivan and Murray (2003) for reduction approaches based on the master equation).

6. Feedback control of surface roughness

The production of high-quality thin films requires that the surface roughness is maintained at a desired level. In this work, we consider as manipulated variable the substrate temperature which is assumed to change only with respect to time. This is a reasonable formulation for the manipulated input and is practically feasible for many experimental and industrial deposition processes. With such a manipulated input formulation, the only variable that can be controlled is a spatially averaged roughness, as defined in Eq. (16). We could have formulated a control problem under the assumption that a large number of manipulated inputs (control actuators) are available to control surface roughness with higher precision but such a control problem formulation would not be practically feasible at the present time. As we will see below, it is possible by manipulating substrate temperature (single input formulation) to achieve an overall very smooth surface configuration.

The fact that the model that describes the evolution of the thin film growth process is not available in closed form (MC model) motivates the use of a proportional-integral (PI) feedback controller to regulate the surface roughness. Specifically, the controller has the following form:

$$u(\tau) = K_c \left[(\hat{y} - y_{\text{set}}) + \frac{1}{\tau_c} \int_0^{\tau} (\hat{y} - y_{\text{set}})\, \mathrm{d}t \right], \tag{21}$$

where y_{set} is the set-point for the controlled output, $\hat{y}$ is the output of the roughness estimator, K_c is the proportional gain and τ_c is the integral time constant. The reader may refer to Lou and Christofides (2003) for results on multivariable controller design for surface roughness and growth rate control in the same thin film process.

The PI controller is coupled with the roughness estimator presented in the previous section. A diagram of the closed-loop system under the proposed estimator/controller structure is shown in Fig. 9. The roughness estimator includes the MC model which uses a reduced-order lattice, the adaptive filter and the measurement error compensator. The output of the MC model is sent to the adaptive filter (Eq. (17)) to suppress the noise, and the measurement error compensator (Eqs. (19) and (20)) updates the filtered roughness based on the measurements. Finally, the roughness estimates are used in the PI controller to determine the substrate temperature.

A closed-loop simulation was run to evaluate the effectiveness of the estimator/controller structure. The size of the reduced-order lattice is 20×20, and a 50×50 lattice

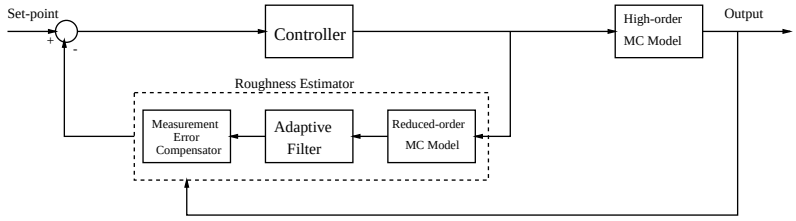

Fig. 9. Diagram of the closed-loop system.

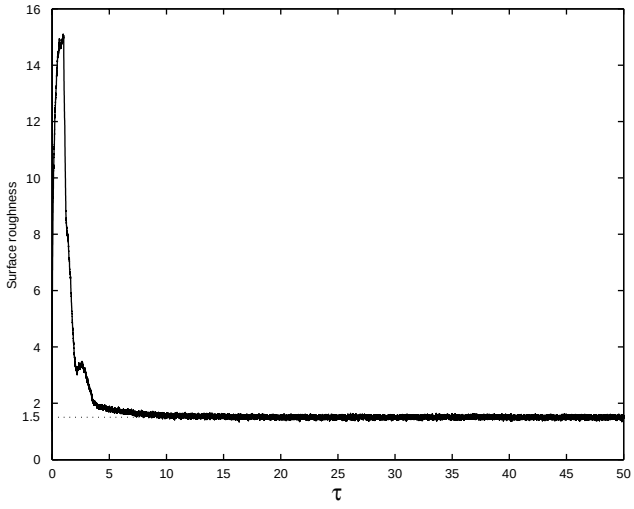

Fig. 10. Evolution of the surface roughness under feedback control based on the roughness estimator.

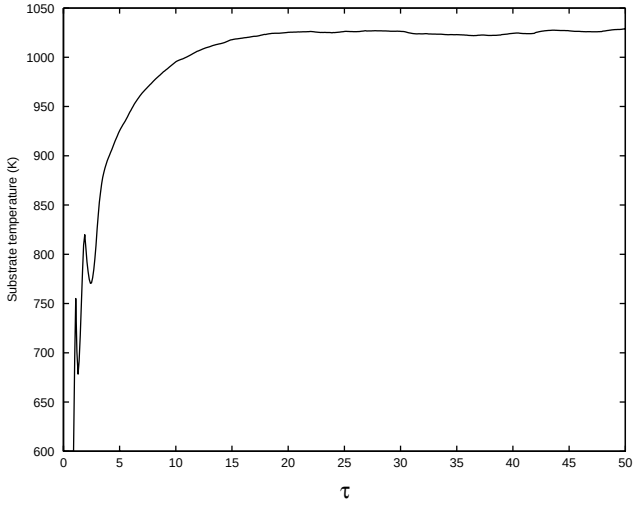

Fig. 11. The evolution of the substrate temperature based on the roughness estimator.

MC model is used to describe the evolution of the process. The desired roughness is 1.5. The time interval between two available measurements is 0.3 s; this is consistent with spectroscopic ellipsometry techniques that can be used to measure surface roughness on-line (Zapien et al., 2001). Other parameters used in the PI simulation are shown in Table 1.

Initially, the thin film grows on a perfect surface at $T = 600$ K and the roughness increases. Then, the controller is activated when the roughness reaches 15.5. Fig. 10 shows the evolution of surface roughness under feedback control. Fig. 11 shows the profile of the substrate temperature. The results clearly show that the proposed estimator/controller structure can successfully drive the surface roughness to the desired set-point value.

The micro-configurations of the surface before the controller is activated and at the end of the closed-loop simulation run are shown in Figs. 12 and 13, respectively. The controller successfully reduces the surface roughness of the thin film.

To test the robustness of the proposed estimator/controller structure, we considered controlling the thin film growth process in the presence of 10% uncertainty in the energy associated with a single bond on the surface. Figs. 14 and 15 show the corresponding output and input profiles, respectively. The controller exhibits very good robustness properties (compare Figs. 10 and 14).

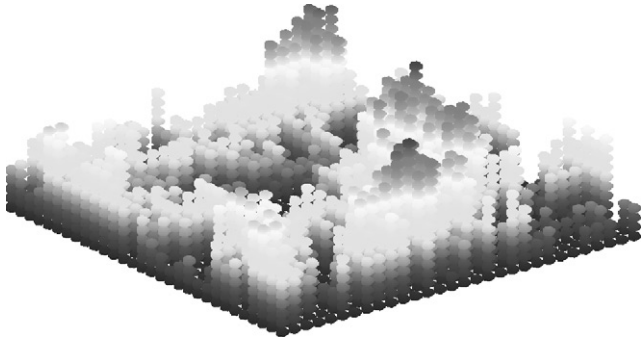

Fig. 12. The micro-configuration of the surface for $T = 600$ K.

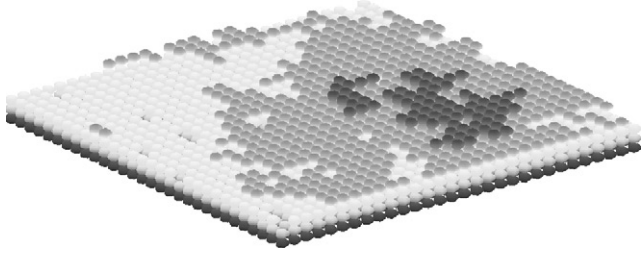

Fig. 13. The micro-configuration of the surface at the end of the closed-loop simulation run—feedback control based on the roughness estimator.

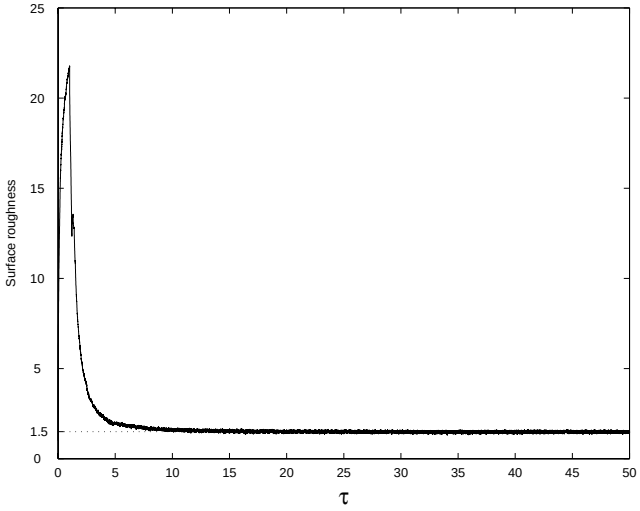

Fig. 14. Evolution of the surface roughness under feedback control based on the roughness estimator—closed-loop system simulation under uncertainty.

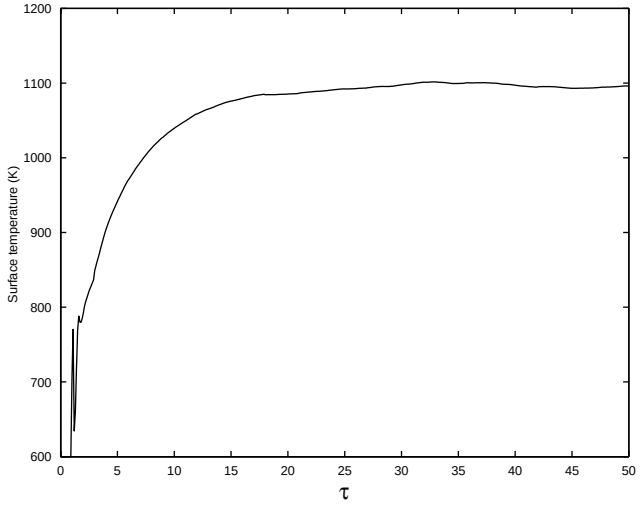

Fig. 15. Evolution of the substrate temperature under feedback control based on the roughness estimator—closed-loop system simulation under uncertainty.

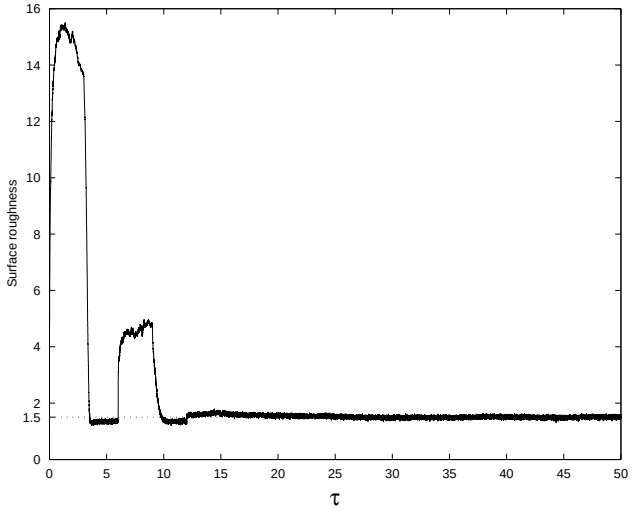

Fig. 16. Evolution of the surface roughness under feedback control without roughness estimator.

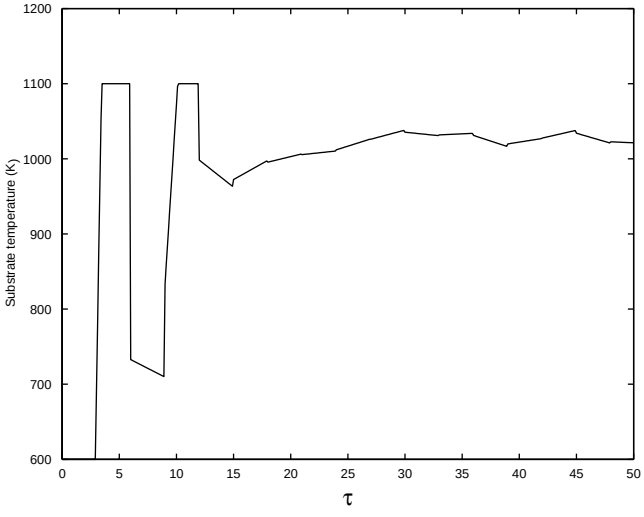

Fig. 17. Evolution of the substrate temperature under feedback control without roughness estimator.

To show the importance of using the roughness estimator for feedback control and not relying exclusively on the roughness measurements (which are obtained every 0.3 s), we applied the PI controller (with the same parameters as in Table 1) to the multiscale process model assuming that new roughness measurements are fed into the controller every 0.3 s (this is consistent with our previous simulations). Also, to prevent the substrate temperature from increasing to an unreasonably high value, the substrate temperature is constrained to be below $T_{\max} = 1100$ K. We note that when the roughness is controlled using the proposed controller/estimator structure, the substrate temperature is always lower than $T_{\max}$ (see Fig. 11). Figs. 16 and 17 show the evolution of surface roughness and substrate temperature, respectively. Due to the discrete measurements, we observe significant oscillations in the surface roughness profile; this simulation shows the usefulness of the proposed estimator/controller structure.

Remark 2. We note that the fundamental reason for the poor performance shown in Fig. 16 is that the discrete measurements cannot capture the full dynamics of the system, which prevents efficient control actions to be computed by the controller. Tuning the controller cannot achieve a control performance as good as that achieved under feedback control using the roughness estimator. As shown in Fig. 16, when the controller is tuned to achieve fast dynamics in the output, significant oscillation can be seen in the

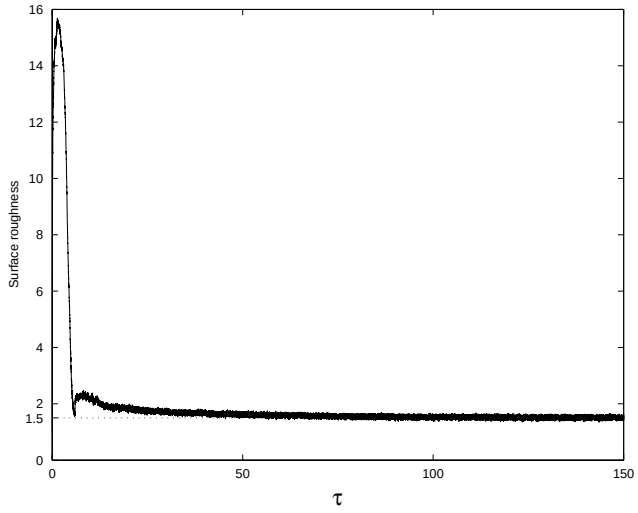

Fig. 18. Evolution of the surface roughness under feedback control without roughness estimator: controller is tuned such that significant oscillation is avoided.

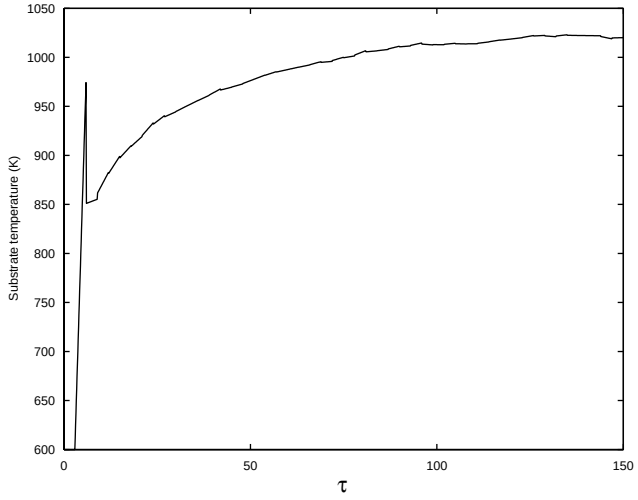

Fig. 19. Evolution of the substrate temperature under feedback control without roughness estimator: controller is tuned such that significant oscillation is avoided.

roughness profile. The oscillations could be reduced by tuning the controller; however, the result of this is that the time needed for the process to reach the steady state becomes much longer. To show this, we applied the PI controller with a set of new parameters ($K_c = 10,\ \tau_c = 1.0$) to the same multiscale process model assuming that the new roughness measurements are fed into the controller every 0.3 s. The parameters of the PI controller are tuned to avoid significant oscillation in the roughness profile under feedback control. Figs. 18 and 19 show the profiles of surface roughness and substrate temperature, respectively. With the new controller parameters, fewer oscillations are observed, but the process takes significantly longer time to reach the new steady state (compare Figs. 11 and 19; in Fig. 11, the substrate temperature reaches the steady-state value at around $\tau = 20$, but in

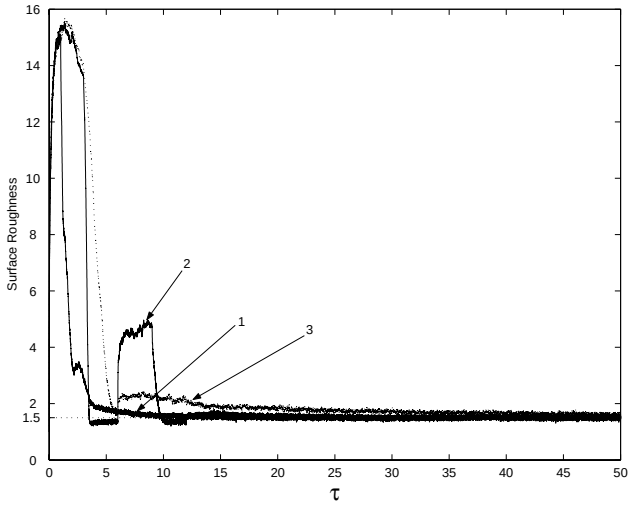

Fig. 20. Comparison of roughness profiles: (1) roughness profile under feedback control based on the roughness estimator, (2) roughness profile under feedback control without roughness estimator with controller parameters shown in Table 1 and (3) roughness profile under feedback control without roughness estimator with controller parameters tuned to avoid significant oscillation.

Fig. 19, the substrate temperature reaches the steady-state value at around $\tau = 100$). To better compare the performance of the various control approaches, the closed-loop roughness profiles shown in Figs. 10, 16 and 18 are shown together in Fig. 20. We also tried many other sets of turning parameters of the PI controller, but it turns out it is hard to achieve short transient time and less oscillation simultaneously when controlling the surface roughness exclusively relying on the discrete measurements.

Remark 3. Furthermore, when there is time-delay in the measurements of surface roughness, the PI controller (with parameters shown in Table 1) is not able to drive the surface roughness to the set-point value. To show this, we applied the PI controller to the multiscale process model assuming that the new roughness measurements are fed into the controller every 0.3 s with a time-delay of $t_d = 0.3$ s. Also, to prevent the substrate temperature from reaching an unreasonably high or low values, the substrate temperature is constrained to be between $T_{\max} = 1100$ K and $T_{\min} = 300$ K. We note that the lower limit of the substrate temperature $T_{\min} = 300$ K was not reached in any of the previous simulations. Figs. 21 and 22 show the profiles of surface roughness and substrate temperature under PI control using the discrete roughness measurements with time-delay. Due to the existence of time-delay in the measurements, we observe that the PI controller cannot drive the output to the desired set-point value. On the other hand, when the estimator/controller structure is used, the measurement-delay has very little effect to the control performance. To show this, we applied the estimator/controller structure (the parameters of the PI controller are the same

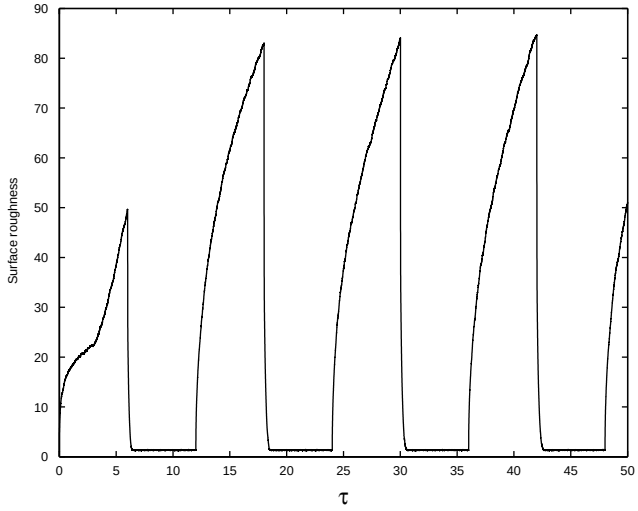

Fig. 21. Evolution of the surface roughness under feedback control without roughness estimator—delayed roughness measurements.

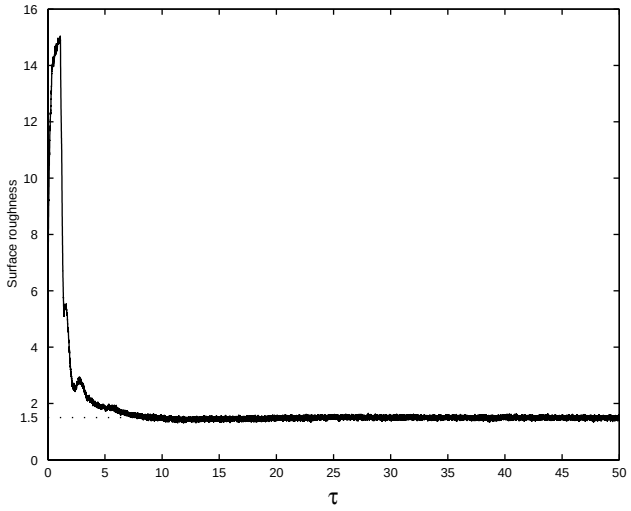

Fig. 23. Evolution of the surface roughness under feedback control based on the roughness estimator—delayed roughness measurements.

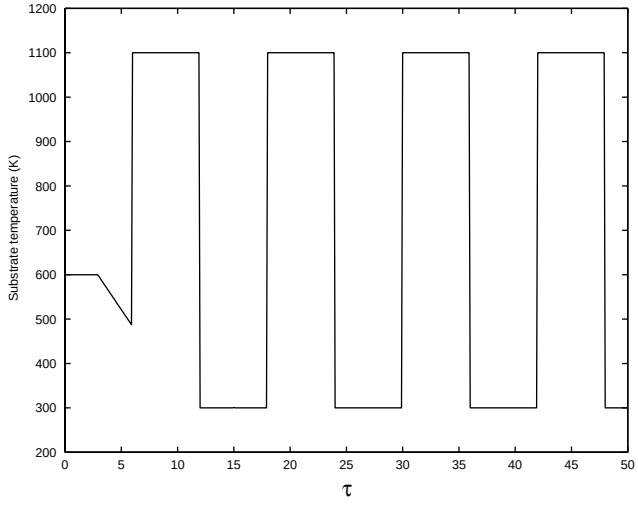

Fig. 22. Evolution of the substrate temperature under feedback control without roughness estimator—delayed roughness measurements.

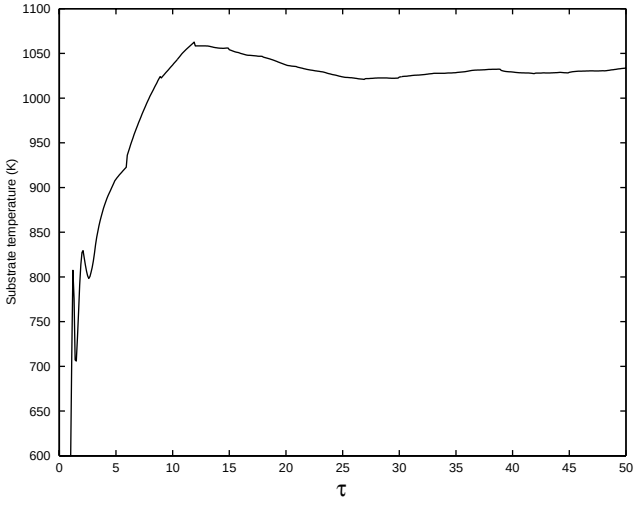

Fig. 24. Evolution of the substrate temperature under feedback control based on the roughness estimator—delayed roughness measurements.

to those shown in Table 1) to the multiscale process model assuming that new roughness measurements are fed into the estimator every 0.3 s with a time-delay of $t_d = 0.3$ s. The resulting profiles of surface roughness and substrate temperature are shown in Figs. 23 and 24. The proposed estimator/controller structure successfully drives the surface roughness to the set-point value in the presence of time-delay in the roughness measurements.

Remark 4. Furthermore, to show that the estimator/controller structure is able to control the surface roughness independently of the frequency at which the roughness measurements are available, we implemented the proposed structure without using roughness measurements, i.e. the controller determines the substrate temperature based only on the output of the kinetic MC simulator which uses the reduced-order lattice and the adaptive filter. Figs. 25 and 26 show the resulting profiles of surface roughness and substrate temperature. Our simulation results show that this open-loop implementation of the proposed controller/estimator structure (with same parameters as those shown in Table 1) successfully drives the surface roughness to the desired value.

Remark 5. The fluctuations of the roughness value obtained by using a reduced-order lattice MC model can be reduced by independently running several MC simulations using a reduced-order lattice with the same parameters and averaging the roughness values obtained from the different runs. Fig. 27 shows a comparison of the evolution of surface

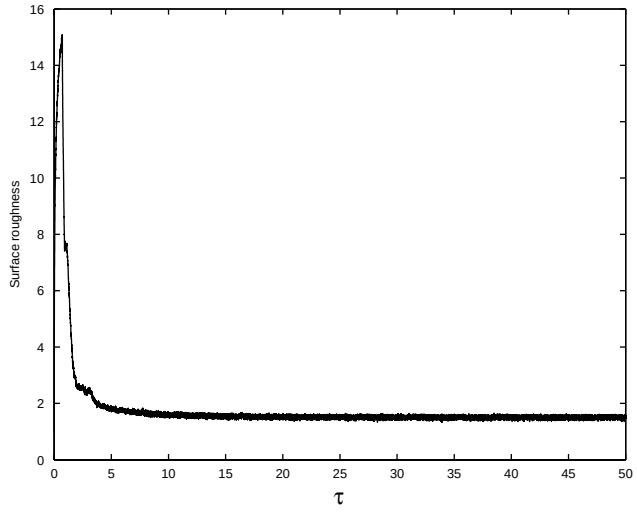

Fig. 25. Evolution of the surface roughness under open-loop implementation of the estimator/controller structure.

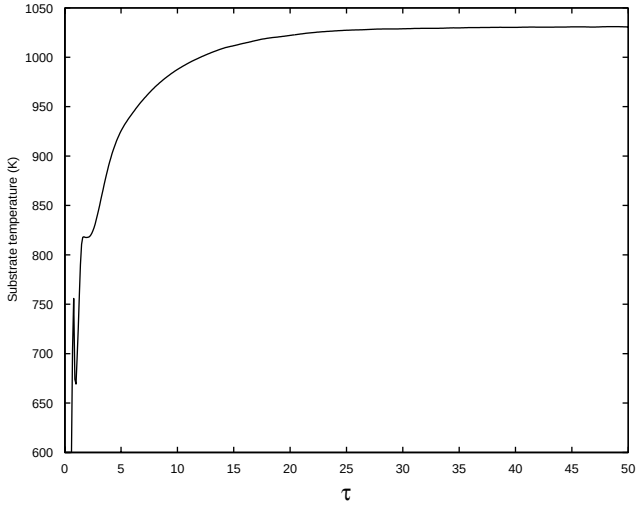

Fig. 26. Evolution of the substrate temperature under open-loop implementation of the estimator/controller structure.

roughness obtained from (a) a kinetic MC simulator which uses a 20×20 lattice, (b) the computation of the average of six independent MC simulations which utilize a 20×20 lattice, and (c) a MC simulator which uses a 100×100 lattice. These results show that when the outputs from multiple reduced-order lattice models are averaged, a more accurate calculation of surface roughness is obtained. However, by increasing the number of MC simulations, the computational requirement is also increasing. For the simulations of Fig. 27, the computational time for the averaged roughness is six times as much as that needed to perform one MC simulation run and it is approximately equal to the computational time needed to run an MC simulation on a 30×30 lattice. Fig. 28 shows a comparison of the evolution of roughness obtained from (a) an MC simulator which uses a 30×30 lattice, (b) the computation of the average of six independent MC simulations which utilize a 20×20 lattice, and (c) an MC simulator which uses a 100×100 lattice. The results of Fig. 28 show that the roughness obtained by averaging six MC simulations, which use a 20×20 lattice model, is close to the one obtained from the 100×100 lattice model and is superior to the one obtained from the 30×30 lattice model.

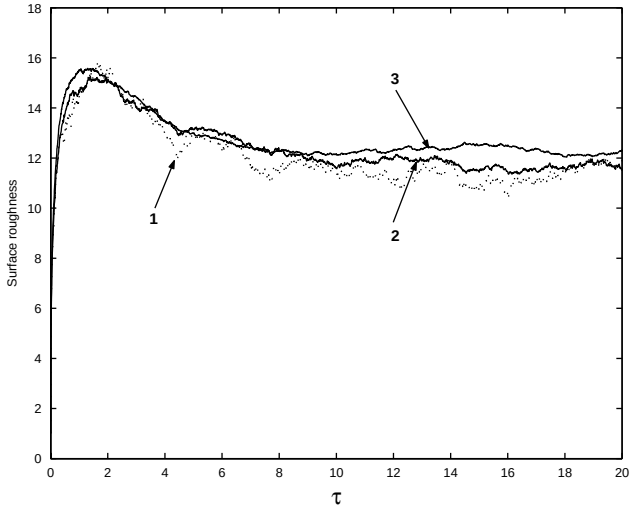

Fig. 27. Comparison of the evolution of roughness from: (1) an MC simulator which uses a 20×20 lattice, (2) the computation of the average of six independent MC simulations which utilize a 20×20 lattice, and (3) an MC simulator which uses a 100×100 lattice.

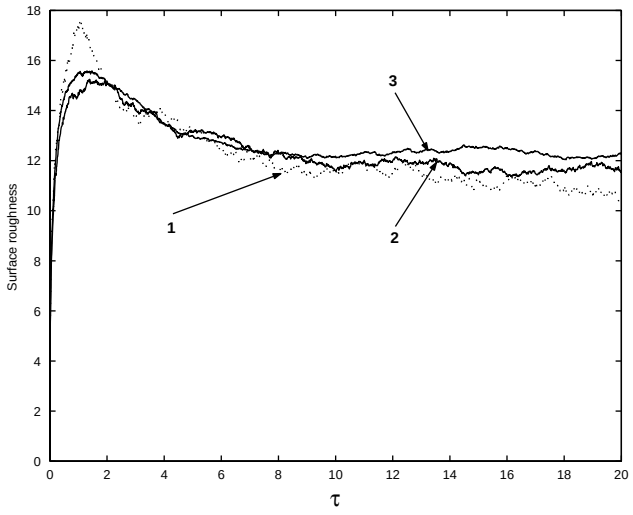

Fig. 28. Comparison of the evolution of roughness from: (1) an MC simulator which uses a 30×30 lattice, (2) the computation of the average of six independent MC simulations which utilize a 20×20 lattice, and (3) an MC simulator which uses a 100×100 lattice.

Fig. 29 shows the evolution of surface roughness under feedback control using a roughness estimator based on a kinetic MC simulator which employs six reduced-order lattice models. Fig. 30 shows the corresponding profile of the substrate temperature. The results are comparable to the case of

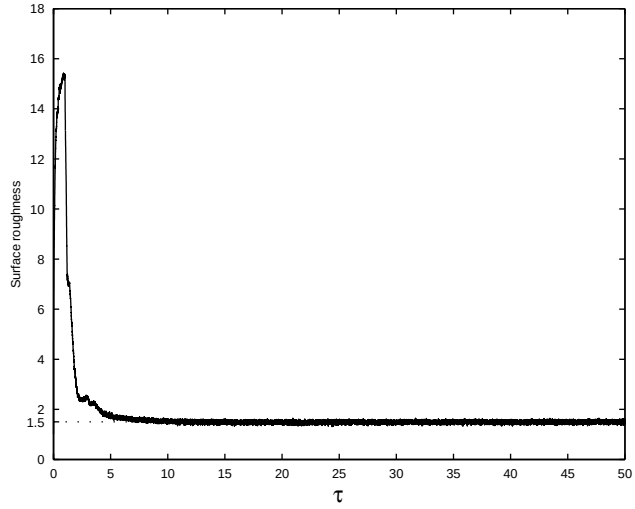

Fig. 29. Evolution of the surface roughness under feedback control using a roughness estimator based on a kinetic MC simulator that employs six reduced-order lattice models.

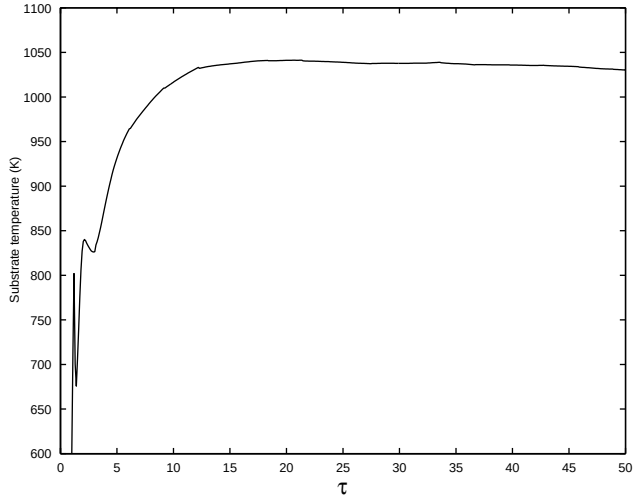

Fig. 30. Evolution of the substrate temperature under feedback control using a roughness estimator based on a kinetic MC simulator that employs six reduced-order lattice models.

using a kinetic MC simulator which uses one 20×20 lattice in the controller (compare closed-loop roughness profiles in Figs. 10 and 29); which means that the feedback control system based on a kinetic MC simulator which uses a single reduced-order lattice performs very well.

7. Conclusions

This work proposed an approach to estimation and control of surface roughness in thin film growth. A feedback control system, which can be implemented in real time, was developed and applied to a thin film growth process in a stagnation flow geometry. The control system consists of a roughness estimator and a proportional integral controller. The roughness estimator combines kinetic Monte Carlo simulator that uses reduced-order lattice model, a filter and a measurement error compensator that uses discrete roughness measurements. Application of the proposed estimator/controller structure to the multiscale process model demonstrates successful regulation of the surface roughness at the desired set-point value. The proposed approach is shown to be superior to PI control with direct use of the discrete roughness measurements. The reason is that the available measurement techniques do not provide measurements at a time-scale comparable to the evolution of the dominant film growth dynamics. We finally note that although the effectiveness of proposed control method is demonstrated through application to a thin-film growth process in a stagnation flow geometry, the method can be applied to other processes described by multiscale distributed models to control microscopic phenomena.

Acknowledgements

Financial support from the National Science Foundation, CTS-002626, is gratefully acknowledged.

References

Akiyama, Y., Imaishi, N., Shin, Y. S., & Jung, S. C. (2002). Macro- and micro-scale simulation of growth rate and composition in MOCVD of yttria-stabilized ziroconia. *Journal of Crystal Growth*, *241*, 352–362.

Armaou, A., & Christofides, P. D. (1999). Plasma-enhanced chemical vapor deposition: Modeling and control. *Chemical Engineering Science*, *54*, 3305–3314.

Armaou, A., Siettos, C. I., & Kevrekidis, I. G. (2002). Time-steppers and control of microscopic distributed processes. *A.I.Ch.E. Annual Meeting*, Paper 257a, Indianapolis, IN, 2002.

Baker, J., & Christofides, P. D. (1999). Output feedback control of parabolic PDE systems with nonlinear spatial differential operators. *Industrial and Engineering Chemistry Research*, *38*, 4372–4380.

Chabal, Y. J., Muller, D. A., Opila, R. L., Kwo, J. R., Busch, B. W., Pluchery, O., & Garfunkel, E. (2002). *MRS Bulletin*, *3*, 206–211.

Chang, J. P., Lin, Y. S., Berger, S., Kepten, A., Bloom, R., & Levy, S. (2001). Ultrathin zirconium oxide films as alternative gate dielectrics. *Journal of Vacuum Science Technology B*, *19*, 2137–2143.

Chen, S., Merriman, B., Kang, M., Caflisch, R. E., Ratsch, C., Cheng, L. T., Gyure, M., Fedkiw, R. P., & Osher, S. (2001). A level set method for thin film epitaxial growth. *Journal of Computational Physics*, *167*, 1–26.

Christofides, P. D. (2001). *Nonlinear and robust control of PDE systems: Methods and applications to transport-reaction processes*. Boston: Birkhäuser.

Fichthorn, K. A., & Weinberg, W. H. (1991). Theoretical foundations of dynamical Monte Carlo simulations. *Journal of Chemical Physics*, *95*, 1090–1096.

Gadgil, P. N. (1993). Single wafer processing in stagnation point flow CVD reactor: Prospects, constraints and reactor design. *Journal of Electronic Materials*, *22*, 171–177.

Gallivan, M. A., Goodwin, D. G., & Murray, R. M. (2001). Modeling and control of thin film morphology using unsteady processing parameters: Problem formulation and initial results. In *Proceedings of 40th IEEE conference on decision and control*, Orlando, FL, USA (pp. 1570–1576).

Gallivan, M. A., & Murray, R. M. (2003). Model reduction and system identification of master equation control systems. In *Proceedings of American control conference*, Denver, CO.

Gilmer, G. H., & Bennema, P. (1972). Simulation of crystal growth with surface diffusion. *Journal of Applied Physics*, *43*, 1347–1360.

Granneman, E. H. (1993). Thin films in the integrated circuit industry: Requirements and deposition methods. *Thin Solid Films*, *228*, 1–11.

Jansen, A. P. J. (1995). Monte Carlo simulations of chemical reactions on a surface with time-dependent reaction-rate constants. *Computer Physics Communications*, *86*, 1–12.

Kang, H. C., & Weinberg, W. H. (1992). Dynamic Monte Carlo simulations of surface-rate processes. *Accounts of Chemical Research*, *25*, 253–259.

Lam, R., & Vlachos, D. G. (2001). Multiscale model for epitaxial growth of films: Growth mode transition. *Physical Review B*, *6403*, 396–404.

Lee, Y. H., Kim, Y. S., Ju, B. K., & Oh, M. H. (1999). Roughness of ZnS : Pr, Ce/Ta_2O_5 interface and its effects on electrical performance of alternating current thin-film electroluminescent devices. *IEEE Transactions on Electronics Devices*, *46*, 892–896.

Lou, Y., & Christofides, P. D. (2003). Feedback control of growth rate and surface roughness in thin film growth. *A.I.Ch.E. Journal*, in press.

Ni, D., Lou, Y., Christofides, P. D., Lao, S., & Chang, J. P. (2003). Real-time feedback control of carbon content of zirconium dioxide thin films using optical emission spectroscopy. In *Proceedings of the international symposium on advanced control of chemical processes*, Hong Kong, China.

Raimondeau, S., & Vlachos, D. G. (2000). Low-dimensional approximations of multiscale epitaxial growth models for microstructure control of materials. *Journal of Computational Physics*, *160*, 564–576.

Reese, J. S., Raimondeau, S., & Vlachos, D. G. (2001). Monte Carlo algorithms for complex surface reaction mechanisms: Efficiency and accuracy. *Journal of Computational Physics*, *173*, 302–321.

Theodoropoulou, A., Adomaitis, R. A., & Zafiriou, E. (1999). Inverse model based real-time control for temperature uniformity of RTCVD. *IEEE Transactions on Semiconductors Manufacturing*, *12*, 87–101.

Van Kampen, N. G. (1992). *Stochastic processes in physics and chemistry*. Amsterdam: North-Holland.

Vlachos, D. G. (1997). Multiscale integration hybrid algorithms for homogeneous-heterogeneous reactors. *A.I.Ch.E. Journal*, *43*, 3031–3041.

Voigtländer, B. (2001). Fundamental processes in Si/Si and Ge/Si studied by scanning tunneling microscopy during growth. *Surface Science Reports*, *43*, 127–254.

Wallace, R. M., & Wilk, G. D. (2002). *MRS Bulletin*, *3*, 192–197.

Zapien, J. A., Messier, R., & Collin, R. W. (2001). Ultraviolet-extended real-time spectroscopic ellipsometry for characterization of phase evolution in BN thin films. *Applied Physics Letters*, *78*, 1982–1984.

Ziff, R. M., Gulari, E., & Barshad, Y. (1986). Kinetic phase transitions in an irreversible surface-reaction model. *Physics Review Letters*, *56*, 2553–2556.